J|A|C|S
ARTICLES
Published on Web 03/14/2006

# Efficient Ribosomal Peptidyl Transfer Critically Relies on the Presence of the Ribose 2′-OH at A2451 of 23S rRNA

Matthias D. Erlacher,[†] Kathrin Lang,[‡] Brigitte Wotzel,[†] Renate Rieder,[‡] Ronald Micura,*[,‡] and Norbert Polacek*[,†]

*Contribution from the Innsbruck Biocenter, Division of Genomics and RNomics-Innsbruck Medical University, Fritz-Pregl Strasse 3, 6020 Innsbruck, Austria, and Center for Molecular Biosciences Innsbruck (CMBI), Institute of Organic Chemistry, Leopold Franzens University, Innrain 52a, 6020 Innsbruck, Austria*

Received December 31, 2005; E-mail: ronald.micura@uibk.ac.at; norbert.polacek@i-med.ac.at

***Abstract:*** The ribosomal peptidyl transferase center is a ribozyme catalyzing peptide bond synthesis in all organisms. We applied a novel modified nucleoside interference approach to identify functional groups at 9 universally conserved active site residues. Owing to their immediate proximity to the chemical center, the 23S rRNA nucleosides A2451, U2506 and U2585 were of particular interest. Our study ruled out U2506 and U2585 as contributors of vital chemical groups for transpeptidation. In contrast the ribose 2′-OH of A2451 was identified as the prime ribosomal group with potential functional importance. This 2′-OH renders almost full catalytic power to the ribosome even when embedded into an active site of six neighboring 2′-deoxyribose nucleosides. These data highlight the unique functional role of the A2451 2′-OH for peptide bond synthesis among all other functional groups at the ribosomal peptidyl transferase active site.

## Introduction

Peptidyl transfer is the fundamental process of protein synthesis with amide bond formation as the crucial chemical reaction and is catalyzed within the ribosomal peptidyl transferase center (PTC) of the large (50S) ribosomal subunit (Figure 1A). Biochemical and recent crystallographic studies revealed that the PTC is composed entirely of 23S rRNA (ref 1 and reviewed in ref 2), and consequently, catalysis of peptide bond formation is based on a ribozyme mechanism, yet to be revealed in its molecular details. In the crystallographic structure of the 50S subunit two ribosomal groups were seen within hydrogen-bonding distance to the attacking α-amino group of aminoacyl-tRNA, namely the adenine N3 and the ribose 2′-OH of A2451 (Figure 1B).[1,3] A prominent hypothesis proposes that the N3 of the universally conserved A2451 (*E. coli* numbering is used here and throughout the manuscript) is involved in acid−base catalysis and functions as a proton acceptor.[1] Although many aspects of the initial model did not survive the scrutiny of subsequent experimental testing (refs 4−8 and reviewed in ref 2), A2451 remained the prime suspect for a catalytic nucleotide even though other highly conserved residues, such as U2506, U2585, or A2602, are also in close proximity to the active site of the PTC. Among those residues U2585 and A2602 received special attention since these were the structurally most flexible nucleotides within the PTC in response to substrate binding and have been proposed to be of functional relevance for translation (ref 9 and reviewed in ref 2). While the complete deletion of A2602 had only marginal effects on transpeptidation and hence excludes this residue for providing crucial functional groups for amide bond formation,[10] the role of U2585 and U2506 remained unclear. One way to experimentally test the functional roles of these 23S rRNA nucleotides involves the generation of site-specific chemically modified ribosomes with retained functionality. Owing to the huge size and complexity of rRNAs such an undertaking seemed impossible thus far. This problem was overcome here by applying a novel approach (the gapped-cp-reconstitution) that allows the site-specific incorporation of non-natural nucleoside analogues into 23S rRNA of *Thermus aquaticus* 50S subunits (Figure 1A). This approach is used in the following to target the mechanistic role of A2451, U2506, and U2585 in peptide bond formation and to clearly identify the functional groups involved.

The gapped-cp-reconstitution system is based on the use of circularly permuted (cp) 23S rRNA for 50S assembly. The cp-

[†] Division of Genomics and RNomics-Innsbruck Medical University.
[‡] Leopold Franzens University.

(1) Nissen, P.; Hansen, J.; Ban, N.; Moore, P. B.; Steitz, T. A. *Science* **2000**, *289*, 920−930.
(2) Polacek, N.; Mankin, A. S. *Crit. Rev. Biochem. Mol.* **2005**, *40*, 285−311.
(3) Hansen, J. L.; Schmeing, T. M.; Moore, P. B.; Steitz, T. A. *Proc. Natl. Acad. Sci. U.S.A.* **2002**, *99*, 11670−11675.
(4) Polacek, N.; Gaynor, M.; Yassin, A.; Mankin, A. S. *Nature* **2001**, *411*, 498−501.
(5) Thompson, J.; Kim, D. F.; O'Connor, M.; Lieberman, K. R.; Bayfield, M. A.; Gregory, S. T.; Green, R.; Noller, H. F.; Dahlberg, A. E. *Proc. Natl. Acad. Sci. U.S.A.* **2001**, *98*, 9002−9007.
(6) Katunin, V. I.; Muth, G. W.; Strobel, S. A.; Wintermeyer, W.; Rodnina, M. V. *Mol. Cell* **2002**, *10*, 339−346.
(7) Youngman, E. M.; Brunelle, J. L.; Kochaniak, A. B.; Green, R. *Cell* **2004**, *117*, 589−599.
(8) Beringer, M.; Bruell, C.; Xiong, L.; Pfister, P.; Katunin, V. I.; Mankin, A. S.; Böttger, E. C.; Rodnina, M. V. *J. Biol. Chem.* **2005**, *280*, 36065−36072.
(9) Bashan, A.; Agmon, I.; Zarivach, R.; Schlünzen, F.; Harms, J.; Berisio, R.; Bartels, H.; Franceschi, F.; Auerbach, T.; Hansen, H. A.; Kossoy, E.; Kessler, M.; Yonath, A. *Mol. Cell* **2003**, *11*, 91−102.
(10) Polacek, N.; Gomez, M. G.; Ito, K.; Nakamura, Y.; Mankin, A. S. *Mol. Cell* **2003**, *11*, 103−112.

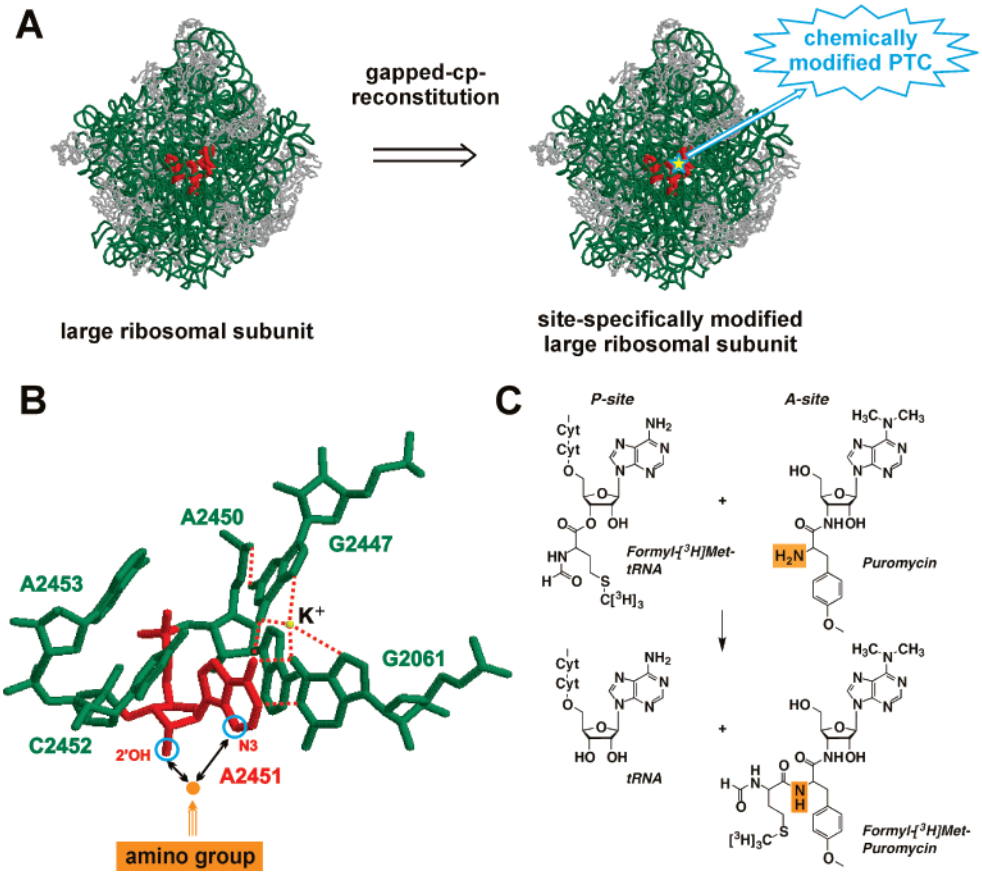


***Figure 1.*** The ribosomal peptidyl transferase center (PTC). (A) The crystallographic structure of the *H. marismortui* large ribosomal subunit viewed from the interface side (left). The 23S rRNA and 5S rRNA are shown as green ribbons, and ribosomal proteins are in gray. The PTC is highlighted by nucleotides of the 23S rRNA peptidyl transferase loop shown in red. Applying the "gapped-cp-reconstitution" approach allows us to site-specifically place a chemically modified nucleoside inside the PTC (right). (B) View of the active site of the PTC structure. The distance between the nitrogen atom of the attacking amino group of an aminoacyl-tRNA analogue (orange sphere) and the N3 or the ribose 2′-OH of A2451 (red) are indicated by black arrows. Tertiary interactions are depicted by red dotted lines. (A) and (B) were generated from pdb files 1FFK and 1FG0,[1] respectively. (C) The standard puromycin reaction.[32] The α-amino group (orange) of A-site bound puromycin attacks the ester bond of P-site bound formyl-[$^3$H]-Methionine-tRNA$^{fMet}$. For the P-site bound tRNA only the 3′ CCA-aminoacyl fragment is depicted.

23S rRNAs were generated by covalently connecting the natural ends of 23S rRNA and introducing new endpoints at appropriate positions in the PTC, thereby placing gaps in the 23S rRNA sequence encompassing the nucleoside under investigation. This missing rRNA segment was chemically synthesized and used in consort with the cp-23S rRNA to reconstitute 50S subunits (Figure 2A). Even though the applied technique has the advantage of performing modified nucleoside interference studies in the ribosome, its intrinsic limitations have to be considered.[10,11] Importantly, transpeptidation in reconstituted large ribosomal subunits proceeds clearly slower than the known in vivo rate of ~15 $s^{-1}$ (see Materials and Methods). Therefore this experimental system is not applicable to measure subtle changes in transpeptidation but turned out to be valuable to pinpoint crucial groups in the PTC whose chemical modification significantly hampered the overall rate of the reaction. In addition, the gapped-cp-reconstitution is not very efficient, and compared to full length 23S rRNA transcripts only 10−20% of cp-23S rRNA assembled into active particles (ref 11 and data not shown). Within the limits of our experimental system, we recently showed that base modifications at A2451, including those which eliminate the proton acceptor capabilities at N3, only marginally affected the transpeptidation rates in the puromycin reaction (Figure 1C).[11] Even the deletion of the entire nucleobase, by placing a ribose-abasic site analogue at position 2451, was largely tolerated. However, the additional removal of the ribose 2′-OH, thereby generating a deoxy-abasic site, markedly inhibited amide bond synthesis. Comparing the activities of these two abasic variants suggested that the 2′-OH at A2451 plays an important role in catalytic activities of the PTC.[11]

## Results and Discussion

Elimination of the entire nucleobase at A2451 is a rather invasive modification destroying multiple interactions with other highly conserved residues in the PTC (Figure 1B). It has been shown by others that results of active site mutants that disrupt tertiary interactions are difficult to interpret.[12] We therefore intended to further substantiate our hypothesis of the A2451 2′-OH being involved in peptide bond formation by synthesis and incorporation of 3-deaza-2′-deoxyadenosine at position 2451 (Figure 2B; see also Materials and Methods). The advantage of 3-deaza-2′-deoxyadenosine is that it eliminates both potential proton acceptors at A2451 simultaneously and yet maintains

(11) Erlacher, M. D.; Lang, K.; Shankaran, N.; Wotzel, B.; Hüttenhofer, A.; Micura, R.; Mankin, A. S.; Polacek, N. *Nucleic Acids Res.* **2005**, *33*, 1618−1627.

(12) Hesslein, A. E.; Katunin, V. I.; Beringer, M.; Kosek, A. B.; Rodnina, M. V.; Strobel, S. A. *Nucleic Acids Res.* **2004**, *32*, 3760−7370.

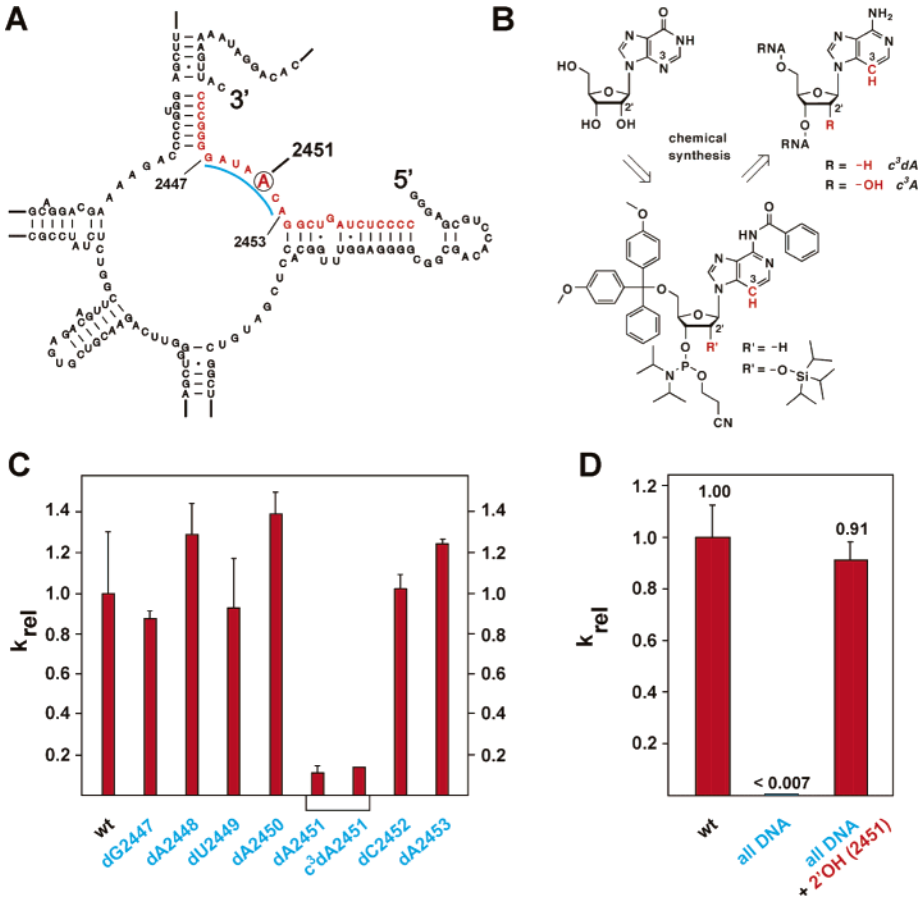


***Figure 2.*** Modified nucleoside interference probing of the PTC. (A) Secondary structure of the PTC of gapped-cp-reconstituted 50S subunits showing the new endpoints of the cp-23S rRNA at positions 2468 and 2440 (5′ and 3′, respectively). The chemically synthesized 26-nucleotide RNA, which compensates for the missing rRNA segment, is shown in red. The region where modified nucleosides have been introduced is underlined in blue. (B) Chemical synthesis of 3-deaza-2′-deoxyadenosine ($c^3$dA) and 3-deazaadenosine ($c^3$A) containing RNA (Supporting Information; see also Schemes 1 and 2).[26] (C) Relative initial peptidyl transferase rates ($k_{rel}$) in the puromycin reaction (ref 11) of ribosomes carrying the synthetic RNA fragment with the wild-type sequence (wt), single 2′-deoxyribose nucleosides at the indicated positions (d), or the $c^3$dA analogue at 2451 (Supplemental Table 1). (D) Relative initial rates of ribosomes containing seven 2′-deoxyribose nucleosides from positions G2447 to A2453 (all DNA) or the same 26-mer with a single 2′-OH reintroduced at position A2451 (all DNA + 2′-OH (2451)) in the puromycin reaction. The $k_{rel}$ values are given above the respective bars. The rate of ribosomes containing the "all DNA" oligo could not be measured at the early time points and was therefore estimated to be <0.007 compared to the wt. The initial rates in (C) and (D) were determined from points in the linear range of the reaction within the first 10 min of incubation. Values shown represent the mean and standard deviation of at least two time-course experiments.

all the other functional groups of adenosine. This allowed us for the first time to investigate the catalytic performance of a PTC where the two prime suspects for crucial functional ribosomal groups were modified concurrently without decisively destroying the active site architecture. If the N3 of A2451 participates in transpeptidation, introducing 3-deaza-2′-deoxyadenosine would add to the harmful effect of the 2′-deoxyadenosine modification. However, the removal of the second potential proton acceptor did not additionally inhibit peptide bond formation in the standard puromycin assay (Table 1 and Figure 2C). This finding, combined with N3 removal alone having little effect,[11] underlines that the main inhibition stems from the elimination of the ribose 2′-OH at A2451 and indicates that the contribution of the nucleobase to catalysis is only minor.

It has recently been demonstrated that the minimal A-site substrate puromycin is hypersensitive to active site changes.[7] To test the performance of chemically modified ribosomes with substrates that better mimic the in vivo situation, we employed here a peptidyl transferase assay using full-length tRNAs. Even though the reduced activities of 50S subunits containing 2′-deoxyribose modifications at 2451 in general could be marginally rescued using genuine aminoacyl-tRNA, the activities were still reproducibly weaker compared to the corresponding ribose variants (Table 1 and Supplemental Figure 3). These data emphasize the critical role of the ribose 2′-OH at A2451 for transpeptidation independent of the A-site substrate used.

To investigate possible functional implications of U2585 or U2506 in transpeptidation, we constructed cp-23S rRNAs that allow placing 2′-deoxyuridine or a ribose-abasic site at these inner shell residues (Figure 3). Our data showed that none of those modifications had an inhibitory effect on peptide bond synthesis in both the puromycin and the full-length tRNA assay (Table 1). In fact, the abasic 2585 and 2506 variants reproducibly showed slightly accelerated reaction rates in the puromycin assay. This contrasts results employing 50S subunits carrying natural base mutations at U2585 or U2506 which showed moderate to strong reductions in transpeptidation using in vitro assembled (ref 10 and data not shown) or in vivo derived particles.[7] Removal of the entire nucleobase at these positions obviously eliminates the structural distortions that are likely present in the A, C, or G mutants which in turn allows a more unrestricted accommodation of puromycin in the A-site. This conclusion is supported by recent crystallographic structures suggesting that for efficient peptide bond formation the nucleo-

***Table 1.*** Activities of Chemically Modified Ribosomes in the Puromycin (Pmn) Reaction and in a Two tRNA Peptidyl Transferase Assay

| | | Pmn reaction | two tRNA assay |
|---|---|---|---|
| 23S rRNA position | modification | $k_{rel}$[a] | $k_{rel}$[a] |
| wt | none | 1.00 | 1.00 |
| A2451 | $c^3$A | 0.77[b] | 0.81 |
| | $c^3$dA | 0.15 | 0.22 |
| | dA | 0.11[b] | 0.20 |
| | d-abasic | <0.01[b] | 0.05 |
| | r-abasic | 0.53[b] | 0.50 |
| U2585 | dU | 1.03 | 1.17 |
| | r-abasic | 1.49 | 0.91 |
| U2506 | dU | 0.99 | 0.91 |
| | r-abasic | 2.21 | 0.97 |

[a] Initial transpeptidation rate ($k_{rel}$) of ribosomes carrying the wild-type (wt) synthetic RNA-oligomer was taken as 1.00 and compared to ribosomes containing modified nucleoside analogues at positions A2451, U2585, or U2506. $k_{rel}$ were determined from experimental points in the linear range of the reactions (Supplemental Figure 3). [b] Data taken from ref 11. Tested nucleoside analogues: 3-deazaadenosine ($c^3$A), 3-deaza-2′-deoxyadenosine ($c^3$dA), 2′-deoxyadenosine (dA), 2′-deoxyuridine (dU), 2′-deoxyabasic (d-abasic), or the ribose-abasic site analogue (r-abasic).

bases at U2506 and U2585 have to move away in the activated PTC to create space for an optimal positioning of the attacking α-amino group of the A-site substrate relative to the peptidyl-tRNA ester.[13] In this way, the abasic U2585 and U2506 ribosomes seem to mimic the activated state of the PTC and therefore accelerate the puromycin reaction.

Introduction of a single DNA nucleoside into the catalytic center can theoretically inhibit the activity of ribozymes by impeding the fine-tuning of the productive conformational state or by changing the overall hydrogen bonding potential.[14] To investigate the requirement of ribose 2′-hydroxyl groups in the PTC in a thorough manner, we individually introduced DNA residues at every position of the synthetic RNA neighboring A2451, which is not involved in Watson−Crick interactions (Figure 2A). The placement of 2′-deoxyribose nucleosides at all tested positions did not compromise peptide bond formation, with the single exception of A2451 (Figure 2C). This clearly demonstrates that the inhibitory effect of the 2′-OH removal is specific for A2451. Simultaneous removal of all 2′-hydroxyls from positions G2447 to A2453 reduced the activity below the detection limit (Figure 2D and Supplementary Figure 4). Significantly, reimplantation of a single 2′-OH at A2451 almost completely restored full transpeptidation activity (Figure 2D). The fact that this sole 2′-OH renders essentially full activity even when surrounded by six 2′-deoxyribonucleosides makes the scenario of a misfolded PTC upon DNA residue insertions less plausible. In a previous in vivo study using snoRNA-guided methylation, the modification of the A2451 2′-OH resulted in a lethal growth phenotype in yeast.[15] One possible explanation for this in vivo result could be ribosome assembly defects upon ribose methylation at this site. To investigate whether the A2451 2′-OH modification compromised the 50S assembly in our in vitro system we have previously compared the sucrose gradient profiles of "wild type" and 2′-deoxy-A2451 50S subunits, which turned out to be indistinguishable.[11] More importantly, "wild type" and 2′-deoxy-A2451 ribosomes showed full activities in

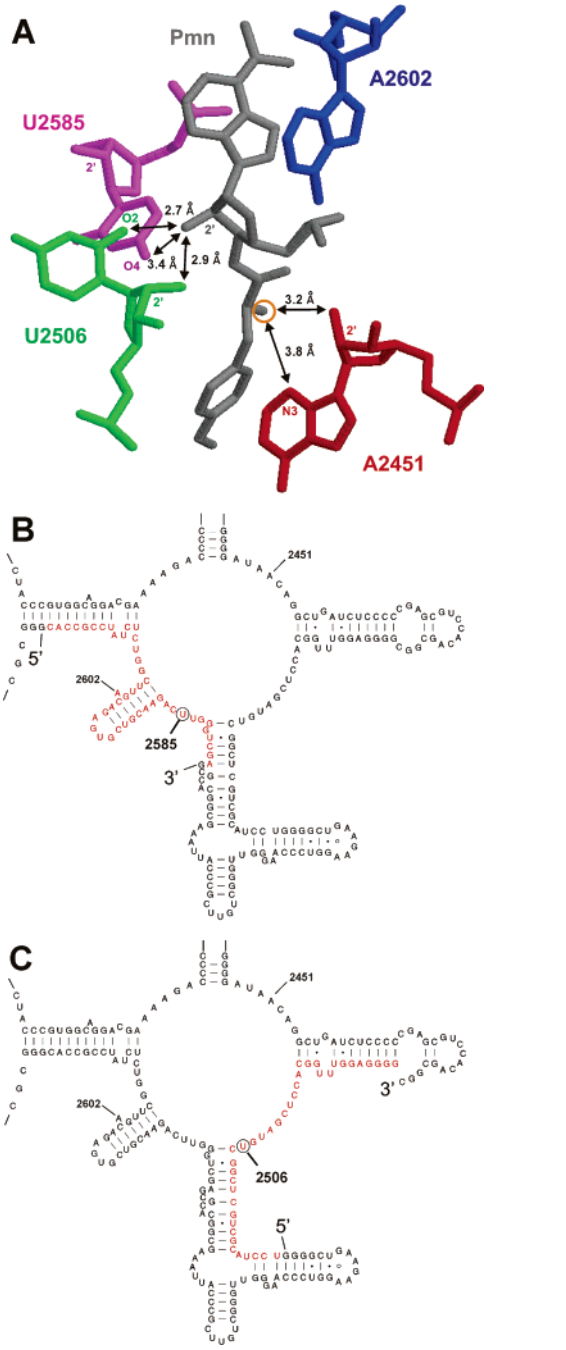


***Figure 3.*** Chemical mutagenesis at U2585 and U2506. (A) Structure of the inner shell residues A2451 (red), U2506 (green), U2585 (magenta), and A2602 (blue). Distances between functional groups of the 23S rRNA residues to the A-site-bound puromycin (Pmn) are indicated by black arrows. The position of the nitrogen atom of the attacking amino group is encircled in orange. The figure was generated from pdb file 1FG0.[1] (B, C) Secondary structures of the PTC of gapped-cp-reconstituted 50S subunits used to chemically modify U2585 (B) or U2506 (C). The chemically synthesized RNA fragments that are used to fill the gap of the cp-23S rRNA during reconstitution are shown in red.

the second fundamental chemical reaction of the PTC, namely in release factor mediated peptide release.[11] Both, peptide bond formation and peptide release, were shown to be single turnover reactions under our assay conditions, and therefore the peptide release activities suggested that comparable fractions of catalytically active 50S subunits were assembled with the wild-type RNA oligomer or the 2′-deoxy-A2451 variant.[11] These data combined with the new findings presented in Figures 2 and 3

(13) Schmeing, T. M.; Huang, K. S.; Strobel, S. A.; Steitz, T. A. *Nature* **2005**, *438*, 520−524.
(14) Gordon, P. M.; Fong, R.; Deb, S. K.; Li, N.; Schwans, J. P.; Ye, J.; Piccirilli, J. A. *Chem. Biol.* **2004**, *11*, 237−246.
(15) Liu, B.; Fournier, J. *RNA* **2004**, *10*, 1130−1141.

highlight the exceptional functional role of the A2451 2′-OH for peptide bond formation.

Previous studies employing standard mutagenesis failed to unequivocally identify the crucial functional group(s) of 23S rRNA for peptide bond formation.[4−8,12,16] Here we applied a novel approach that allows the chemical modification of single 23S rRNA groups inside the large ribosomal subunit. Within the limits of the experimental system, our chemical mutagenesis study discloses the ribose 2′-OH at A2451 as the prime candidate in the PTC with vital importance to forge an amide bond. The unperturbed p$K_a$ of a ribose 2′-OH is far from neutral and therefore unfavorable to directly participate in acid/base chemistry. We favor the view that the universally conserved A2451 plays a role as a molecular trigger that senses the substrates in the active site and properly aligns its ribose 2′-OH group for coordinating the attacking α-amino group. This interpretation is in line with recent crystallographic data showing the attacking amine to be in hydrogen bonding distance to the A2451 2′-OH in the ground state.[13,17] Alternatively, and even though not seen in the currently available crystal structures from the Steitz and Strobel laboratories,[13,17] the 2′-OH of A2451 could be involved in transition state stabilization. In support of this possibility, a molecular dynamics simulation study was presented that predicts the A2451 2′-OH to be part of a H-bond network that stabilizes the transient tetrahedral intermediate (TI) of peptide bond formation.[18] Removal of the ribose 2′-OH at A2451 was calculated to significantly destabilize the relative free energy of the TI by ∼3 kcal/mol. Irrespective of the specific role of the A2451 2′-OH, it is likely that the evolutionary pressure that conserved the nucleobase identity at this residue ensures correct positioning of its 2′-OH group for efficient peptide bond catalysis. A similarly important role for another universally conserved adenosine has recently been proposed for the 2′-OH of the terminal nucleoside of peptidyl-tRNA.[19,20] The currently available data suggest that effective peptide bond catalysis relies on the presence of two ribose 2′-OH groups; one located in the ribosome (at A2451 of 23S rRNA) and the other on the P-site substrate (at A76 of P-tRNA), rather than on any nucleobase functional group.

## Conclusion

Even though the crystal structures of the ribosome and its individual subunits provide a wealth of detailed insights, the molecular mechanism of peptide bond formation remains controversial and far from being fully understood (reviewed in ref 2). Here we have applied a novel experimental device which allows us to chemically alter functional groups on specific 23S rRNA nucleosides inside the PTC. This modified nucleoside interference approach clearly identified the ribose 2′-OH of A2451 to be of crucial functional importance. The single 2′-OH was necessary and sufficient to provide almost full catalytic power to the PTC, even when introduced into an active site of neighboring 2′-deoxyribose nucleosides. The other potentially functional residues that build the inner shell of the PTC, such as A2602, U2585, or U2506, are not critically required to promote transpeptidation. The data presented here explain why the importance of the A2451 2′-OH escaped the detection by regular mutagenesis studies, since the ribose 2′-OH group remained untouched in all the previous mutants. Our study suggests that the A2451 ribose 2′-OH represents a key functional ribosomal group for effective peptide bond synthesis.

***Scheme 1.*** Synthesis of 3-Deazaadenosine **8**[a]

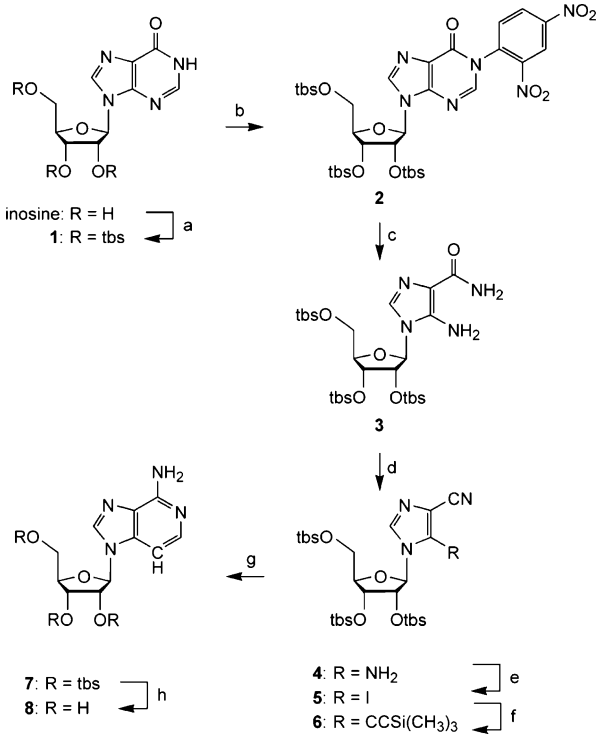


[a] (a) 5 equiv of tbs-Cl, 10 equiv of imidazole in DMF, rt, 20 h, 98%; (b) 2.5 equiv of 2,4-dinitrochlorobenzene, 2.5 equiv of $K_2CO_3$ in DMF, 80 °C, 2.5 h, 93%; (c) ethylenediamine, 50 °C, 6 h, 70%; (d) 1.4 equiv of *p*-toluenesulfonyl chloride in pyridine, rt, 20 h, 95%; (e) 4.1 equiv of isoamyl nitrite in $CH_2I_2$, 100 °C, 45 min, 60%; (f) 4 equiv of ethinyl trimethylsilane, 1.2 equiv of $NEt_3$, 5 mol % $(PhCN)_2PdCl_2$ in $CH_3CN$, 110 °C, 20 h; (g) 7 N $NH_3$/MeOH, 120 °C, 14 h, 50% over two steps; (h) 9 equiv of polymer supported fluoride (Amberlite IRA 900 fluoride-form; macroporous, 20−50 mesh, 3.0 mmol/g loading) in toluene, 110 °C, 6 h, 79%. tbs-Cl = *tert*-butylchlorodimethylsilane; DMF = *N*,*N*-dimethylformamide.

## Materials and Methods

**Syntheses of Phosphoramidite Building Blocks of $c^3$A and $c^3$dA.** The chemical syntheses of 2′-*O*-tris(triisopropylsilyl)-3′-*O*-[(*N*,*N*-diisopropylamino)-(β-cyanoethoxy)phosphino]-5′-*O*-(4,4′-dimethoxytrityl)-$N^6$-benzoyl-3-deazaadenosine **12** ($c^3$A) and of 2′-deoxy-3′-*O*-[(*N*,*N*-diisopropylamino)-(β-cyanoethoxy)phosphino]-5′-*O*-(4,4′-dimethoxytrityl)-$N^6$-benzoyl-3-deazaadenosine **19** ($c^3$dA) started from inosine and proceeded in 12 steps (for $c^3$A) and 15 steps (for $c^3$dA) via the 5-amino-4-imidazolecarboxamide (AICA) riboside derivative **3** (Schemes 1 and 2). Our synthesis strategy took previous reports by Matsuda, Piccialli, McLaughlin, Watanabe, Robins, and their respective coworkers into account.[21−25] Detailed procedures and characterization data are provided in the Supporting Information.

(16) Bayfield, M. A.; Thompson, J.; Dahlberg, A. E. *Nucleic Acids Res.* **2004**, *32*, 5512−5518.
(17) Schmeing, T. M.; Huang, K. S.; Kitchen, D. E.; Strobel, S. A.; Steitz, T. A. *Mol. Cell* **2005,** *20*, 437−448.
(18) Trobro, S.; Aqvist, J. *Proc. Natl. Acad. Sci. U.S.A.* **2005**, *102*, 12395−12400.
(19) Dorner, S.; Panuschka, C.; Schmid, W.; Barta, A. *Nucleic Acids Res.* **2003**, *31*, 6536−6542.
(20) Weinger, J. S.; Parnell, K. M.; Dorner, S.; Green, R.; Strobel, S. A. *Nat. Struct. Mol. Biol.* **2004**, *11*, 1101−1106.
(21) Minakawa, N.; Sasabuchi, Y.; Kiyosue, A.; Kojima, N.; Matsuda, A. *Chem. Pharm. Bull.* **1996**, *44*, 288−295.
(22) DeNapoli, L.; Messere, A.; Montesarchio, D.; Piccialli, G.; Varra, M. *J. Chem. Soc., Perkin Trans. 1* **1997**, 2079−2082.
(23) Bevers, S.; Xiang, G.; McLaughlin, L. W. *Biochemistry* **1996**, *35*, 6483−6490.
(24) Pankiewicz, K.; Matsuda, A.; Watabane, K. A. *J. Org. Chem.* **1982**, *47*, 485−488.

***Scheme 2.*** Synthesis of 3-Deazaadenosine Phosphoramidite **12** and of 2′-Deoxy-3-deazaadenosine Phosphoramidite **19**[a]

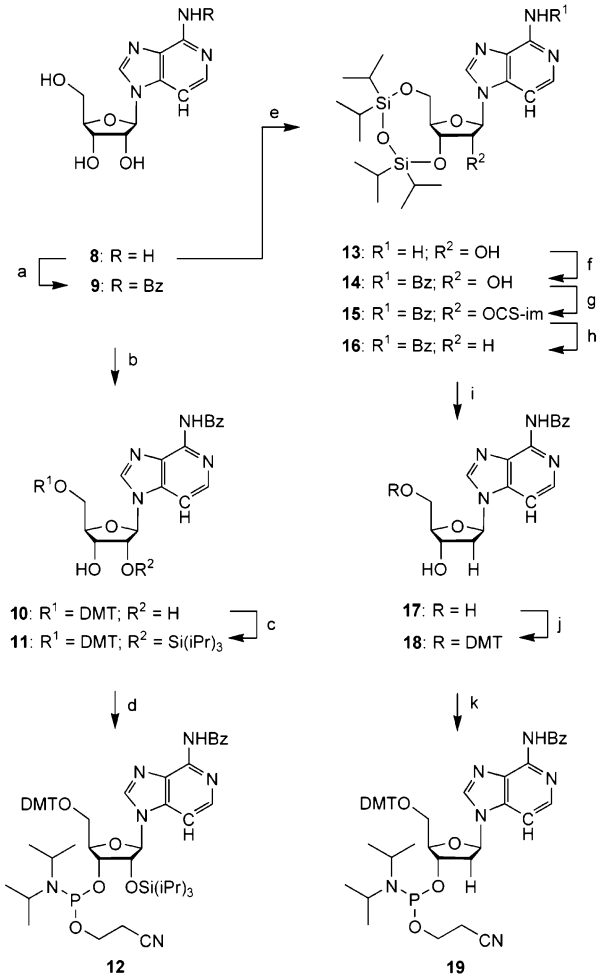


[a] (a) (1) 8.5 equiv of TMS-Cl in pyridine, 0 °C, 50 min; (2) 5.7 equiv of Bz-Cl in pyridine, rt, 3.5 h, 90%; (b) (1) 1.2 equiv of DMF-DMA in pyridine, rt, 1.5 h; (2) 2.7 equiv of DMT-Cl in pyridine, rt, 18 h, 62%; (c) 4 equiv of $AgNO_3$, 3.6 equiv of TIPS-Cl in pyridine/THF, rt, 40 h, 60%; (d) 3.3 equiv of CEP-Cl, 10 eq $Me_2NEt$ in $CH_2Cl_2$, rt, 4 h, 90%; (e) 1.3 equiv of TBDS-$Cl_2$ in pyridine, rt, 5 h, 81%; (f) (1) 5.8 equiv of TMS-Cl in pyridine, 0 °C, 50 min; (2) 6.6 equiv of Bz-Cl in pyridine, rt, 3.5 h, 93%; (g) 1.2 equiv of TCD in DMF, rt, 4 h, 99%; (h) 1.5 equiv of *n*-$Bu_3SnH$, 0.2 equiv of AIBN in toluene, 75 °C, 3 h, 64%; (i) 6 equiv of polymer supported fluoride (Amberlite IRA 900 fluoride-form; macroporous, 20−50 mesh, 3.0 mmol/g loading) in toluene, 110 °C, 5 h, 93%; (j) 1.5 equiv of DMT-Cl in pyridine, rt, 18 h, 49%; (k) 3 equiv of CEP-Cl, 10 equiv of $Me_2NEt$ in $CH_2Cl_2$, rt, 4 h, 80%. TMS-Cl = chlorotrimethylsilane; Bz-Cl = benzoyl chloride; DMF-DMA = *N*,*N*-dimethylformamide dimethylacetal; DMT-Cl = 4,4′-dimethoxytrityl chloride; TIPS-Cl = triisopropylchlorosilane; THF = tetrahydrofuran; CEP-Cl = 2-cyanoethyl-*N*,*N*-diisopropylchlorophosphoramidite; TBDS-$Cl_2$ = 1,3-dichloro-1,1,3,3-tetraisopropyldisiloxane; TCD = 1,1′-thiocarbonyldiimidazole; im = imidazole; AIBN = α,α′-azo-isobutyronitrile.

**Oligoribonucleotide Synthesis, Deprotection, and Purification.** Oligoribonucleotides containing $c^3A$ and $c^3dA$ nucleosides were synthesized using the 2′-*O*-TOM-methodology.[26−29] Details are provided in the Supporting Information.

**Peptidyl Transferase Assays.** Gapped-cp-reconstituted 50S subunits for investigating A2451 were assembled, reassociated with native *T. aquaticus* 30S subunits and subsequently used in the puromycin reaction as described previously.[11] Under these conditions the puromycin reaction with reconstituted 50S containing full-length 23S rRNA transcripts proceeds with a rate of ∼0.6 $min^{-1}$, while ribosomes composed of gapped-cp-reconstituted 50S carrying the wt-oligo sequence promote transpeptidation with a rate of ∼0.012 $min^{-1}$ (data not shown). To investigate U2585 or U2506, cp-23S rRNAs were constructed in analogy to the published procedure.[11] To generate the DNA templates for cp-23S rRNA transcription, the forward and reverse PCR primer pairs *TAATACGACTCACTATA***G**$_{(2523)}$GGGCTGAAGAAGGTCCC and **G**$_{(2483)}$CCGCTGTGGACGCTCGG as well as *TAATACGACTCACTATA***G**$_{(2623)}$GGCGCAGGAGGCTTGAG and **C**$_{(2576)}$GCGTGCCGCTTTAATG were used for the cp-23S rRNA constructs that placed gaps around positions U2506 and U2585, respectively. The T7 promoter sequences in the forward primers are italic, and the positions defining the new 5′ and 3′ ends of the cp-23S rRNAs are bold and numbered according to *E. coli* nomenclature.

To assess the peptidyl transferase activity of reconstituted ribosomes using full-length tRNA substrates, 50S subunits were assembled from 20 pmol cp-23S rRNA and 40 pmol synthetic RNA oligonucleotide as described in ref 11 with the only difference that 8 pmol native *T. aquaticus* 30S subunits were present during the entire reconstitution procedure. Subsequently, the 70S ribosomes were programmed with 60 μg poly(U) and incubated with 3 pmol unlabeled *N*-acetyl-Phe-$tRNA^{Phe}$ for 15 min at 37 °C for P-site binding in a buffer containing 12.1 mM Tris/HCl pH 7.5, 8.4 mM Hepes/KOH pH 7.5, 18.1 mM $MgCl_2$, 5 mM $MnCl_2$, 519 mM $NH_4Cl$, 3.6 mM spermidine, 0.05 mM spermine, 4.1 mM β-mercaptoethanol, and 0.12 mM EDTA. The peptidyl transferase reaction was initiated by the addition of 3 pmol [$^3$H]Phe-tRNAPhe (20 000 cpm/pmol) and performed at 37 °C in a final volume of 46 μL. The reaction was stopped by the addition of 6.1 μL of 10 M KOH and incubation at 37 °C for 15 min. Subsequently 121 μL of 1 M $KH_2PO_4$ and 87 μL of 1 M HCl were added. At this pH value (pH 2.5) the reaction product, *N*-acetyl-Phe-[$^3$H]Phe, can be extracted into ethyl acetate (extraction efficiency was essentially quantitative) and was analyzed by liquid scintillation counting. At this pH unreacted [$^3$H]Phe carries a positive charge and is not coextracted with the dipeptidyl product to a significant extent. In control experiments with 3 pmol completely hydrolyzed [$^3$H]Phe-tRNAPhe (20 000 cpm/pmol), only 400 cpm could be extracted into the organic phase. In peptidyl transferase reactions the background activity (usually ∼500 cpm) that results from possible minor 50S contaminations of the *T. aquaticus* 30S subunit preparation was subtracted from all experimental time points. Compared to the standard puromycin reaction employing gapped-cp-reconstituted 50S, the transpeptidation rate in this full-length tRNA assay was accelerated to ∼0.05 $min^{-1}$. $tRNA^{Phe}$ (Sigma) was aminoacylated using PheRS as described in ref 30, acetylated using acetic anhydride (see ref 31), and HPLC purified according to ref 11.

**Acknowledgment.** We thank Alexander Mankin, Sean Connell, Daniel Wilson, and Karl Grubmayr for valuable suggestions. N.P. thanks Alexander Hüttenhofer for generous support. This work was supported by the Austrian Science Foundation FWF (P16932 and P18709 to N.P.; P17864 to R.M.), the bm: bwk (GEN-AU Project cluster 'Non-coding RNAs'), and the "Tiroler Wissenschaftsfonds" (UNI-404/109 to N.P. and UNI-404/39 to R.M.).

(25) Robins, M. J.; Wilson, J. S.; Hansske, F. *J. Am. Chem. Soc*. **1983**, *105*, 4059−4065.
(26) Micura, R. *Angew. Chem., Int. Ed.* **2002**, *41*, 2265−2269.
(27) Pitsch, S.; Weiss, P. A.; Jenny, L.; Stutz, A.; Wu, X. *Helv. Chim. Acta* **2001**, *84*, 3773−3795.
(28) Höbartner, C.; Kreutz, C.; Flecker, E.; Ottenschläger, E.; Pils, W.; Grubmayr, K.; Micura, R. *Monatshefte für Chemie − Chemical Monthly* **2003**, *134*, 851−873.
(29) Höbartner, C.; Rieder, R.; Kreutz, C.; Puffer, B.; Lang, K.; Polonskaia, A.; Serganov, A.; Micura, R. *J. Am. Chem. Soc*. **2005**, *127*, 12035−12045.
(30) Polacek, N.; Swaney, S.; Shinabarger, S. D.; Mankin, A. S. *Biochemistry* **2002**, *41*, 11602−11610.
(31) Triana-Alonso, F. J.; Spahn, C. M.; Burkhardt, N.; Rohrdanz, B.; Nierhaus, K. H., *Methods Enzymol.* **2000**, *317*, 261−276.
(32) Monro, R. E.; Marcker, K. A. *J. Mol. Biol*. **1967**, *25*,347−350.

**Supporting Information Available:** Synthetic procedures and characterization data of 3-deaza-adenosine **12** and 3-deaza-2′-deoxyadenosine phosphoramidites **19** for RNA solid-phase synthesis. Supplemental Figures 1−4 and Supplemental Table 1. This material is available free of charge via the Internet at http://pubs.acs.org.

JA0588454